

Profile of bile acids-FXR-FGF15 pathway in the glycolipid metabolism disorder of diabetic mice suffered with chronic stress

Weijia Cai^{1,2}, Canye Li^{1,2}, Zuanjun Su^{1,2}, Jinming Cao^{1,2}, Zhicong Chen^{1,2}, Yitian Chen^{1,2}, Zhijun Guo³, Feng Xu^{Corresp. 1,2}

¹ Fengxian Hospital and School of Pharmaceutical Sciences, Southern Medical University, Shanghai, China

² Sixth People's Hospital South Campus, Shanghai Jiaotong University, Shanghai, China

³ Heyou Meihe Hospital, Foshan, Guangdong, China

Corresponding Author: Feng Xu
Email address: xuf@smu.edu.cn

Background. The development of diabetes and depression is related to imbalance of bile acids (BAs) synthesis and metabolism in rodents and humans. However, the role of BAs and their receptor FXR (farnesoid X receptor)/FGF15 (Fibroblast Growth Factor 15) signal pathway in diabetes and depression comorbidity remains largely unknown. This study was aimed to investigate the BAs-associated potential molecular mechanisms underlying glycolipid metabolism disorder in diabetic mice suffered with chronic stress. **Methods.** Type 2 Diabetes Mellitus (T2DM) mice model was first induced by high-fat diet and intraperitoneal injection of streptozotocin (STZ). Forty mice were randomly divided into two groups: the normal chow feeding group and the high-fat diet feeding group. After 2 weeks of feeding, the mice were therefore randomly divided into 4 groups: Control group, CUMS group, T2DM group, and T2DM+CUMS group. The T2DM group and T2DM+CUMS groups were intraperitoneal injection of STZ to induce T2DM model. The CUMS and T2DM+CUMS groups were exposed with chronic unpredictable mild stress (CUMS) to induce depression-like phenotype. Blood and tissue samples were obtained for relevant analysis and detection. **Results.** Compared with T2DM group mice, T2DM+CUMS group mice had higher blood glucose and lipid levels, insulin resistance, inflammation of the liver and pancreas, meanwhile further impaired liver function, and increased total bile acids. These changes were accompanied by inhibition of FXR signaling. Compared to those in T2DM group mice, chronic stress more inhibited FXR expression and its downstream target FGF15 in the ileum. **Conclusion.** FXR might play a role in diabetic glycolipid metabolism disorder aggravated by chronic stress. FXR and its downstream target FGF15 might be therapeutic targets for T2DM and depression comorbidity treatment.

1 **Profile of Bile Acids-FXR-FGF15 Pathway in the**
2 **Glycolipid Metabolism Disorder of Diabetic Mice**
3 **Suffered with Chronic Stress**

4
5
6 **Weijia Cai^{1,2}, Canye Li^{1,2}, Zuanjun Su^{1,2}, Jinming Cao^{1,2}, Zhicong Chen^{1,2}, Yitian Chen^{1,2},**
7 **Zhijun Guo³ and Feng Xu^{1,2*}**

8
9

10 ¹ Fengxian Hospital and School of Pharmaceutical Sciences, Southern Medical University,
11 Shanghai, China

12 ² Sixth People's Hospital South Campus, Shanghai Jiaotong University, Shanghai, China

13 ³ Heyou Meihe Hospital, Foshan, Guangdong, China

14

15 Corresponding Author:

16 Feng Xu¹

17 Sixth People's Hospital South Campus, Shanghai Jiaotong University, 6600 Nanfeng Hwy,
18 Shanghai, 201499, China

19 Email address: xuf@smu.edu.cn

20

21 **Abstract**

22 **Background.** The development of diabetes and depression is related to imbalance of bile acids
23 (BAs) synthesis and metabolism in rodents and humans. However, the role of BAs and their
24 receptor FXR (farnesoid X receptor)/FGF15 (Fibroblast Growth Factor 15) signal pathway in
25 diabetes and depression comorbidity remains largely unknown. This study was aimed to
26 investigate the BAs-associated potential molecular mechanisms underlying glycolipid
27 metabolism disorder in diabetic mice suffered with chronic stress.

28 **Methods.** Type 2 Diabetes Mellitus (T2DM) mice model was first induced by high-fat diet and
29 intraperitoneal injection of streptozotocin (STZ). Forty mice were randomly divided into two
30 groups: the normal chow feeding group and the high-fat diet feeding group. After 2 weeks of
31 feeding, the mice were therefore randomly divided into 4 groups: Control group, CUMS group,
32 T2DM group, and T2DM+CUMS group. The T2DM group and T2DM+CUMS groups were
33 intraperitoneal injection of STZ to induce T2DM model. The CUMS and T2DM+CUMS groups
34 were exposed with chronic unpredictable mild stress (CUMS) to induce depression-like
35 phenotype. Blood and tissue samples were obtained for relevant analysis and detection.

36 **Results.** Compared with T2DM group mice, T2DM+CUMS group mice had higher blood
37 glucose and lipid levels, insulin resistance, inflammation of the liver and pancreas, meanwhile
38 further impaired liver function, and increased total bile acids. These changes were accompanied

39 by inhibition of FXR signaling. Compared to those in T2DM group mice, chronic stress more
40 inhibited FXR expression and its downstream target FGF15 in the ileum.

41 **Conclusion.** FXR might play a role in diabetic glycolipid metabolism disorder aggravated by
42 chronic stress. FXR and its downstream target FGF15 might be therapeutic targets for T2DM
43 and depression comorbidity treatment.

44 Introduction

45 According to a report by the International Diabetes Federation (IDF), 10.5% (537 million) of the
46 world will have diabetes in 2021 and it is expected to increase to 12.2% (783 million) by 2045
47 (Sun et al. 2022). Among them 30-40% of patients with diabetes will develop at least one
48 complication within 10 years. Traditionally complications associated with diabetes include
49 macrovascular disease as well as microvascular disease (Viigimaa et al. 2020). Currently, as
50 people with diabetes live longer and longer, new complications emerge, including cancer,
51 infections, psychological and mental disorders (Harding et al. 2019a). Patients with diabetes are
52 at increased risk for major depression (Ali et al. 2006), anxiety (Fisher et al. 2008), and serious
53 mental illnesses such as schizophrenia (Vancampfort et al. 2016). One in 4 patients with type 2
54 diabetes will develop major depression. Patients with diabetes usually have a higher risk of
55 depression compared to those with normal blood glucose (Semenkovich et al. 2015). A
56 systematic review concluded that the mean prevalence of depression in patients with type 2
57 diabetes was 28% (Harding et al. 2019b), compared with a global prevalence of depression of
58 approximately 13% in the general population (Lim et al. 2018).

59

60 Many factors contribute to the development of diabetes and depression comorbidity. These
61 factors include not only common pathophysiologic factors, but also social and psychological
62 factors, such as financial burden of treatment, fear of disability due to the disease, and strict
63 dietary control or exercise requirements (Pettrak et al. 2015). Additionally, patients with diabetes
64 who developed depression comorbidity often present poorer long-term glycemic control
65 (Heckbert et al. 2010), non-compliance with medical treatment (Lin et al. 2006), and poorer
66 metabolic control (Egede & Ellis 2010).

67

68 The diabetes and depression comorbidity has been recognized as an emerging global challenge
69 (Fisher et al. 2012). Therefore, it is very important to study the pathogenesis of diabetes and
70 depression comorbidity. Currently, the role of bile acids (BAs) in development of many diseases
71 has become a hot topic. Bile acids are proved to be important signaling molecules that can act in
72 various tissues of the body and participate in regulating the body's glucolipid metabolism and
73 homeostasis (Perino & Schoonjans 2022). The bile acid receptor FXR (or NR1H4), and other
74 ligand-activated nuclear receptors (pregnancy X receptor, vitamin D receptor and the membrane
75 receptor TGR5) may all be involved in bile acid signaling (Sun et al. 2018).

76

77 Evidence documented that the development of either diabetes or depression is related to the bile
78 acid signaling pathway. On the one side, there is an increased tendency of serum total bile acid

79 (TBA) levels in patients with type 2 diabetes compared to the normal population (Sonne et al.
80 2016). The serum bile acid concentrations were significantly higher in type 2 diabetic patients
81 than those in the non-diabetic population and displayed a positive correlation with insulin
82 resistance (Sun et al. 2016). The postprandial plasma concentrations of single bile acids and
83 FGF19 were significantly increased in type 2 diabetic patients compared to non-type 2 diabetic
84 patients (Sonne et al. 2016). Bile acids regulate glucose homeostasis by acting directly on FXR
85 and TGR5 in the intestine, liver, and pancreas as well as by promoting FXR and inducing
86 intestinal FGF15/19. FXR inhibits hepatic glycolysis and lipogenesis and reduces postprandial
87 glucose utilization (Caron et al. 2013; Duran-Sandoval et al. 2005; Watanabe et al. 2004a). FXR
88 and FGF15 play an important role in the development of diabetes (Yan et al. 2021).

89
90 On the other side in the last years it has become increasingly evident that bile acids affect brain
91 function, during normal physiological and pathological conditions (Mertens et al. 2017).
92 Although bile acids may be synthesized locally in the brain (Kiriyama & Nochi 2019), the
93 majority of brain bile acids are taken up from the systemic circulation (Monteiro-Cardoso et al.
94 2021), which are mainly metabolites of the liver and intestinal microbiota. Therefore, bile acids
95 in the systemic circulation can directly or indirectly affect central processes and thus be involved
96 in the neuropathological processes of depression (Lirong et al. 2022).

97
98 In chronic stress-induced depressed rats the serum level of glycocholic acid (GCA) was elevated
99 but that of bile acids (CA) was decreased compared to normal control rats (Zhu et al. 2020). In a
100 clinical study of patients with Crohn's disease (CD), a positive correlation between GCA and
101 both the Zung's Self-Assessment Scale for Anxiety (SAS) and the Self-Rating Scale for
102 Depression (SDS) was observed (Feng et al. 2022). However, inconsistent result has also been
103 reported, with one study showing a significant increase in blood cholic acids (CAs) in a chronic
104 restraint-induced depression model mice (Zhang et al. 2010). Research found that FXR altered
105 the bile acids blood concentration and the composition in the brain through FXR knockout mice,
106 contributing to the regulation of homeostasis of multiple neurotransmitter systems in different
107 brain regions and modulating neurobehavior (Huang et al. 2015). FXR expression was
108 significantly downregulated in the medial prefrontal cortex of chronic social defeat stressed mice
109 (Bao et al. 2021). These studies suggested a role for FXR in the development of depression and
110 could be a potential and novel therapeutic target.

111
112 Notwithstanding, the profile of BAs and their receptor FXR/FGF15 signal pathway in diabetes
113 and depression comorbidity remains largely unknown. This study was aimed to investigate the
114 BAs-associated potential molecular mechanisms underlying glycolipid metabolism disorder
115 aggravated with chronic stress in diabetic mice.

116

117 **Materials & Methods**

118 **Animals**

119 Male 5-week-old C57BL/6 mice (Animal Certificate No.: SCXK (Su) 2020-0009 from Jiangsu
120 Huachuang Sino Pharma Tech Could., Ltd., Jiangsu, China) were used in this study. All of the
121 animals were raised in a standardized animal room (temperature 22 ± 2 °C, lights on from 6
122 a.m.~ 6 p.m.), with free access to clean boiled water and rodent chow.

123

124 **The high fed streptozotocin mice model**

125 After two weeks of acclimation, the C57BL/6 mice were randomly assigned to two groups by
126 random number table, one of which was fed with a chow diet (D12450J, 10% fat, 70%
127 carbohydrate, 20% protein, purchased from Jiangsu Xietong Pharmaceutical Bio-engineering
128 Co., Ltd., Jiangsu, China), and the other a high-fat diet (D12492, 60% fat, 20% carbohydrate,
129 and 20% protein, purchased from Jiangsu Xietong Pharmaceutical Bio-engineering Co., Ltd.,
130 Jiangsu, China). After four weeks, the high-fat diet group received two-doses of streptozotocin
131 (STZ, Sigma-Aldrich Co., St. Louis, Missouri, USA) intraperitoneally (80 mg/kg/d with an
132 interval of two days) in 15 minutes of dissolution according to the adapted protocol(Furman
133 2021). The STZ powder was prepared immediately before use with a 0.1 mol/L, pH 4.5 citric
134 acid-sodium citrate buffer (Shanghai Yuanye Bio-Technology Co., Ltd., Shanghai, China).
135 Diabetes was verified 10 days after the last STZ administration by quantifying blood glucose
136 levels by means of a Contour plus blood glucose monitoring system (Bayer, Leverkusen,
137 Germany) through blood sample obtained from the tail vein. Mice with blood glucose
138 concentrations higher than 13.9 mmol/L were considered to be diabetic and used to establish a
139 chronic unpredictable mild stress (CUMS) model.

140

141 **Chronic unpredictable mild stress protocol and experimental designs**

142 Diabetic mice that met blood glucose requirements were included in the development of a
143 depression model, which was used by CUMS to induce a depression-like phenotype in C57BL/6
144 mice. The CUMS procedure was adapted from the protocol (Nollet 2021). Briefly, it lasted for
145 four weeks after the T2DM model was established, with diverse randomly assigned stressors:
146 Damp sawdust for 24 hours; no sawdust for 24 hours; cage tilting for 24 hours; restraint stress
147 for 2 hours; cycle disturbances; swimming at 4 °C for 5 minutes; cage vibration for 20 minutes;
148 noise interference for 1.5 hours. During the stress procedure, two unexpected stressors were
149 performed per day, and no single stressor was performed consecutively for two days. Appendix-
150 table 1 shows the schedule of the stressors. Every mouse subjected to CUMS were housed
151 separately in single cage, and others were housed in groups. After four weeks of CUMS, the
152 mice were divided into four groups: Control, CUMS, T2DM, and T2DM+CUMS (n=10 per
153 group). Fifty mice were utilized for this study and forty were included. Ten mice were excluded,
154 including eight mice which did not meet the blood glucose requirements and another three mice
155 were exclude because of technical failure during CUMS treatment.

156

157 **Validation of CUMS mice model**

158 **Open field test**

159 The mice (n=10 per group) were placed into the open-field chambers with a video capture
160 system (50×50×40 cm³, L×W×H) from the same position in turn, and Tracking master V3.0
161 software (Beijing Zhongshi Dichuang Technology Development Co., Ltd., Beijing, China) was
162 opened to automatically record the mice's activities inside the chamber for 5 minutes. To avoid
163 odor interference, the chambers were sprayed with 75% ethanol after each mouse test.
164 Throughout the experiment, the light in the room was kept consistent and quiet.

165 **Tail suspension test**

166 The mice (n=10 per group) were attached to the hook with medical tape at 3/4 of the tail and
167 suspended in an inverted suspension position. The suspended mouse was about 30 cm from the
168 chamber's bottom, with a camera placed at the level of the suspension device. Tracking master
169 V3.0 software (Beijing Zhongshi Dichuang Technology Development Co., Ltd., Beijing, China)
170 was launched, and the immobility time of the mice in the last 4 minutes of 6 minutes was
171 automatically recorded.

172 **Forced swimming test**

173 The mice (n=10 per group) were placed in a cylindrical bucket with a diameter of 10 cm and a
174 height of 25 cm, and the water level in the bucket was such that the mice could stretch their
175 entire bodies without their tails touching the bottom of the bucket (the water temperature was
176 23~25°C, and the water level was 15 cm high). Tracking master V3.0 software (Beijing
177 Zhongshi Dichuang Technology Development Co., Ltd., Beijing, China) was initiated, and the
178 mice's immobility time in the last 4 minutes within 5 minutes was recorded (the mice were
179 considered immobile when they were floating on the water surface and their limbs were not
180 moving or their limbs were slightly paddling).

181 **Sucrose preference test**

182 During the experiment, each animal (n=10 per group) would be given two identical bottles: one
183 containing clean boiled water and the other containing a 1% sucrose solution. Following the 15h
184 test, liquid consumption was measured. Sucrose preference proportion = sucrose solution
185 consumption / (sucrose solution consumption + boiled water consumption) ×100%.

186

187 **Sacrifice and samples collection**

188 Mice were sacrificed under anesthesia with 4% chloral hydrate after the behavioral tests were
189 completed. Blood was collected, coagulated at room temperature for 30 minutes, and centrifuged
190 at 3000 rpm for 15 minutes.

191

192 The supernatant serum was separated and divided into several vials before being stored at -80°C.
193 Livers and ilea were dissected and immediately frozen in liquid nitrogen after cardiac perfusion.
194 The liver was weighed before being cut into two parts, one fixed with cold 4% paraformaldehyde
195 and the other flash frozen and stored at -80 °C, while the pancreas was fixed with cold 4%
196 paraformaldehyde. Serum samples would be tested for serum lipids, liver function, and insulin
197 levels. Western blotting was performed on frozen livers and ilea. Immunohistochemistry was
198 performed on fixed livers and pancreas.

199

200 Serum lipids and liver function

201 Serum levels of glutamic oxaloacetic transaminase (ALT), glutamic alanine transaminase (AST),
202 total cholesterol (CHO), triglycerides (TG), high-density lipoprotein (HDL), low-density
203 lipoprotein (LDL), non-esterified fatty acid (NEFA), and blood glucose (GLU) were measured
204 by a Beckman Coulter biochemical analysis system (AU5800).

205

206 Enzyme-linked immunosorbent assays

207 Glycated hemoglobin A1c(GHbA1c) concentrations in lysate for red blood cell and serum
208 insulin levels were measured by Mouse Glycated Hemoglobin A1c(GHbA1c) ELISA Kit
209 (#CSB-E08141m, CUSABIO, Wuhan, China, <https://www.cusabio.com/>) and Mouse Insulin
210 ELISA kit (#KE10089, Proteintech Group, Inc., Wuhan, China) according to the manufacturer's
211 instructions.

212

213 Western blotting

214 RIPA was used to extract total proteins from liver and ileum samples (n=3 per group), and the
215 extracts were used to detect FXR, SHP, and FGF15 protein expression. Protein concentration
216 was determined using the BCA method (Yoche Biotechnology, Shanghai, China), and proteins
217 were denatured sequentially using gel electrophoresis and wet membrane transfer. After 2 hours
218 of blocking at room temperature, diluted primary antibodies of FXR (1:1000, Cell Signaling
219 Technology, Inc., Boston, USA), FGF15 (1:1000, Santa Cruz Biotechnology, Inc., California,
220 USA), SHP (1:500, ABclonal Technology Co., Ltd., Wuhan, China), GAPDH (1:10,000,
221 ABclonal Technology Co., Ltd., Wuhan, China), and β -actin (1:1000, ImmunoWay
222 Biotechnology, Plano, TX, USA) were added for overnight incubation at 4°C. After recovering
223 the primary antibodies, the membrane was washed three times with TBST (Sangon Biotech,
224 Shanghai, China) for 10 minutes each, and the secondary antibodies (1:5,000, ImmunoWay
225 Biotechnology, Plano, TX, USA) were added to incubate for 1 hour at room temperature. The
226 ECL reagent was used for image development after washing the membrane, and the protein
227 bands were analyzed using Image J software.

228

229 Total RNA extraction and quantification by qPCR

230 TRIzol reagent (Thermo fisher scientific, MA, USA) was used to extract total RNA from mouse
231 liver and ileum tissues (n=3 per group). The products were then reverse transcribed using the
232 Evo M-MLV RT Mix Kit with gDNA Clean for qPCR (AG11728, Accurate Biotechnology,
233 Hunan, Co., Ltd., Hunan, China). qPCR with reverse transcription was performed using the
234 SYBR Green Premix Pro Taq HS qPCR Kit (AG11718, Accurate Biotechnology, Hunan, Co.,
235 Ltd., Hunan, China) on Applied Biosystems Quant Studio 6 Flex apparatus (Thermo fisher
236 scientific, MA, USA), and the Ct values were calculated using the $2^{-\Delta\Delta Ct}$ method to analyze the
237 relative gene expression level. Appendix-table 2 shows the forward and reverse sequences of the
238 qPCR primers that were designed and synthesized (Sangon Biotech, Shanghai, China). All the

239 procedures were carried out in accordance with the manufacturer's instructions. The target gene
240 values were normalized to ACTB and the relative expression levels were displayed as fold
241 changes relative to control group.

242

243 **Histopathological Analysis**

244 Dehydrated liver specimens (n=3-4 per group) were embedded in paraffin, cut into 4~6 μm
245 sections, and stained with H&E for morphological examination. Oil Red O staining revealed
246 lipid deposition in the liver. Frozen liver sections were air-dried at room temperature for 2 hours
247 before being fixed for 5 minutes with 4% paraformaldehyde. To remove excess water, the
248 sections were washed and rinsed in 60% isopropanol. The sections were then incubated in Oil
249 Red O reagents for 10 minutes before being removed from the solution with 60% isopropanol.
250 Hematoxylin was used to stain the nuclei for 5 minutes before washing them with water.

251

252 **Statistical analysis**

253 Graphpad 9.3.0 statistical software was used for the analysis. The experimental data were
254 presented as mean \pm standard error (SEM). All data were analyzed with unpaired two-tailed
255 Student's t-test (for data from two groups) and one-way ANOVA followed by Tukey's multiple
256 comparison post hoc test (for data from more than two groups). A difference of $P < 0.05$ indicates
257 a statistically significant difference.

258

259 **Results**

260 **Type 2 diabetic mice with depression-like phenotype comorbidity model validation**

261 Mice in the experimental group were subjected to 4 weeks of high-fat chow intervention and
262 STZ via intraperitoneal injection after acclimation and randomization to create a T2DM model.
263 The diabetic model mice that met the glycemic requirements were then included in the 4-week
264 CUMS process to establish a depression-like phenotype (Figure 1A).

265

266 Behavioral analysis was used to verify whether the depression-like phenotype was successfully
267 induced in diabetic mice. In the open field test, the distance and duration of activity in the central
268 area were significantly shorter in the CUMS group than in the Control group. However, the
269 T2DM+CUMS group showed shorter distance and duration of activity in the central area and less
270 total traveled distance compared to the T2DM group (Figure 1B). In the tail suspension and
271 forced swimming tests, CUMS mice presented a longer immobility time when compared to the
272 Control group. Mice in the T2DM+CUMS group also exhibited significantly longer immobility
273 time for tail suspension and forced swimming compared to the T2DM group (Figure 1C, D). In
274 the sucrose preference test, CUMS or T2DM mice showed a lower percentage of sucrose
275 preference compared to the Control group, while T2DM+CUMS showed a lower level of sucrose
276 preference compared to CUMS (Figure 1E).

277

278 **Type 2 diabetic mice with depression-like phenotype in glycolipid metabolism**

279 At the end of the CUMS protocol, metabolic measurements in vivo, including body weight,
280 fasting blood glucose and serum lipids (CHO, TG, LDL, HDL, NEFA), were performed to assess
281 the effect of T2DM and depression comorbidity on glycolipid metabolism. All stressed mice had
282 significantly lower body weight gains and unstable blood glucose levels (Figure 2A, C). There
283 was no significant difference in body weight among the four groups of mice, but the body weight
284 of mice in the T2DM group was slightly higher than that in the T2DM+CUMS group (Figure
285 2B). Fasting blood glucose was measured after the CUMS model was established, and it was
286 discovered that T2DM mice had higher blood glucose levels than Control mice. However, there
287 was no significant difference between the mice in the T2DM+CUMS group and the mice in the
288 T2DM group (Figure 2D). When serum lipids were compared, it was discovered that there were
289 lipid disorders among these groups. T2DM was linked to higher levels of serum CHO, LDL,
290 HDL and NEFA (Figure 2E, G-I). Serum CHO, TG, LDL, and NEFA levels were significantly
291 higher in T2DM+CUMS mice than in T2DM mice (Figure 2E-H). In terms of the GHbA1c test,
292 T2DM+CUMS mice had higher GHbA1c levels than CUMS mice, but there was no significant
293 difference when compared to T2DM mice (Figure 2J).

294

295 **Insulin-related indicators and histopathological analysis of the pancreas in type 2 diabetic** 296 **mice with depression-like phenotype**

297 As stated, serum glucose levels in CUMS and T2DM mice were higher than that in Control.
298 Furthermore, the T2DM+CUMS group had higher serum glucose levels than the CUMS or
299 T2DM group (Figure 3A). What's more, in the insulin test, it was easily discovered that in fasting
300 conditions, CUMS mice showed a significant increase in fasting insulin (Figure 3B). Meanwhile,
301 T2DM+CUMS group showed slightly increase than T2DM group (Figure 3B). Although not
302 statistically significant, the HOMA-IR index increased in stressed mice, particularly in the
303 CUMS and T2DM groups when compared to Control mice. T2DM+CUMS mice also had a
304 higher HOMA-IR index than T2DM mice (Figure 3C). For the HOMA- β index, the T2DM
305 group had a lower HOMA- β index than the Control group, but there was no significant
306 difference in HOMA- β index of T2DM+CUMS when compared to T2DM (Figure 3D).

307 The pancreatic histomorphology revealed that the islets of the Control group mice were round or
308 oval cell clusters of various sizes, complete and regular structures, clear edges, and scattered
309 among the pancreatic vesicles, with more cell clusters and abundant β -cells in the islets, uniform
310 in size, full and tightly arranged, whereas the islets of the CUMS group mice were swollen and
311 deformed, with light cytoplasmic staining or vacuolation. The number of islet cell clusters
312 decreased in the T2DM group, along with shrunken islet area, irregular morphology, unclear islet
313 margin, disorganized structure, swollen and deformed islet cells, light or vacuolated cytoplasmic
314 staining, and obvious nuclear consolidation or nuclear loss. Besides that, some of the exocrine
315 gland vesicles were deep inside the islet, whereas in the T2DM+CUMS group, the islet area was
316 severely shrunk, the morphology was irregular, the islet cells were swollen and deformed, and
317 the cytoplasmic staining was light or vacuolated when compared to T2DM mice (Figure 3E).

318

319 **Liver function, total bile acids and histopathological analysis of the liver in type 2 diabetic** 320 **mice with depression-like phenotype**

321 We found that comorbidity aggravated liver steatosis, lobular inflammation by liver pathological
322 analysis (Figure 4A-C). In Control group, hepatic lobules and hepatic cords were irregularly
323 arranged, hepatocytes were unequal in size, hepatocytes were cloudy and swollen, and there was
324 a small amount of inflammatory cell infiltration in the confluent area. Hepatic lobules and cords
325 were irregularly arranged in the CUMS group, hepatocytes were unequal in size, hepatocytes
326 were cloudy and swollen with partial loss of nuclei, and inflammatory cells were infiltrated in the
327 confluent area, indicating moderate lesions. Hepatic lobules and cords were irregularly arranged
328 in T2DM mice, hepatocytes were unequal in size, hepatocytes were degenerated, and balloon-
329 like changes were visible, indicating mild to moderate steatosis. Furthermore, the T2DM+CUMS
330 group had unequally arranged lobules and hepatic cords, as well as hepatocytes that were
331 degenerated and ballooned, indicating moderate to severe steatosis (see Figure 4A). Then, we
332 investigated the effect of comorbidity on liver steatosis and inflammation, but there was no
333 significant difference in inflammation and steatosis scores in the liver of the T2DM+CUMS
334 group compared to the T2DM group. In addition, comorbidity increased lipid accumulation in
335 the liver as assessed by Oil red O staining (Figure 4D, E). Moreover, comorbidity increased the
336 liver/body weight of mice in CUMS group or T2DM group (Figure 4F). We then measured ALT
337 and AST levels in the liver, and comorbidity increased both levels (Figure 4G, H). Total bile acid
338 was determined in four groups, it was higher in T2DM+CUMS group than T2DM group (Figure
339 4I). Taken together, our data suggest that comorbidity worsens liver function, hepatic steatosis
340 and inflammation, as well as increases total bile acids in T2DM.

341

342 **T2DM and depression-like phenotype regulated by FXR/SHP/FGF15**

343 Compared with the T2DM group, the hepatic FXR mRNA level was slightly lower in the
344 T2DM+CUMS group, but the SHP mRNA level was slightly higher in the liver (Figure 5A, B).
345 T2DM+CUMS group had lower protein level of hepatic FXR than T2DM group. However, in
346 the liver, an increasing tendency in the protein level of SHP were found (Figure 5C).
347 The level of ileal FXR mRNA expression was slightly lower in T2DM+CUMS mice than in
348 T2DM mice. In the T2DM+CUMS group, ileal FGF15 mRNA expression was significantly
349 lower than in the T2DM group (Figure 5D, E). When compared to the T2DM group, ileal FXR
350 protein level was significantly lower in the T2DM+CUMS group. Furthermore, it showed that a
351 lower ileal FGF15 protein level in T2DM+CUMS group (Figure 5F).

352

353 **Discussion**

354 The comorbidity of mental and physical diseases is a major challenge in the world of health care.
355 The comorbidity of depression and diabetes is a typical example of mental/physical comorbidity,
356 with the prevalence of which is increasing and likely to continue to increase due to increasing
357 life expectancy and various other causes. Patients with diabetes are prone to have depression
358 during the disease progression, and they tend to have the following characteristics: female

359 gender, younger and/or older age, individuals living alone, poor social support, low
360 socioeconomic status, poor sleep and lack of physical exercises and diet (Agardh et al. 2011;
361 Bădescu et al. 2016; Sartorius 2018). Besides, a systematic review indicated that the prevalence
362 rate of depression is nearly more than twice as high in people with type 2 diabetes (19.1%, range
363 6.5-33% vs. 10.7%, range 3.8-19.4%) compared to those without (Roy & Lloyd 2012). And the
364 growing evidence also showed that depression and type 2 diabetes share a common biological
365 origin, in particular an overactivation of innate immunity leading to a cytokine-mediated
366 inflammatory response with possible abnormalities through the regulation of the hypothalamic-
367 pituitary-adrenal axis (Moulton et al. 2015). Moreover, the development of diabetes and
368 depression is associated with dysregulation of bile acid synthesis and metabolism in rodents or
369 humans (Feng et al. 2022; Lirong et al. 2022; Sonne et al. 2016; Sun et al. 2016; Zhu et al. 2020).
370 As an important component of the liver-gut-brain axis, studies have also confirmed the key role
371 of the bile acid nuclear receptor FXR in diabetes or depression (Bao et al. 2021; Caron et al.
372 2013; Duran-Sandoval et al. 2005; Huang et al. 2015; Watanabe et al. 2004a; Yan et al. 2021). In
373 summary, there exists a strong association between diabetes and depression.

374

375 Although studies indicated that bile acid nuclear receptor FXR might play an important role in
376 diabetes or depression, there are fewer in-depth studies on the liver-gut axis FXR and its target
377 genes SHP and FGF15 regulating the comorbidity of diabetes and depression. Therefore, we set
378 out to elucidate the role of FXR and its target genes SHP and FGF15 in the development of
379 diabetic mice aggravated by chronic stress.

380

381 The C57BL/6 mouse strain is highly sensitive to the metabolic effects of high-fat feeding, and it
382 is a simple model to obtain (Luo J 1998). In addition, the use of STZ restimulation to reduce the
383 number of β cells and further mimic T2DM has been investigated in the past (Gilbert et al. 2011;
384 Podrini et al. 2013; Shao et al. 2014). In this study, we successfully established a T2DM mice
385 model using 4-week high-fed diet combined with STZ (i.p.). T2DM mice were continued to the
386 establishment of CUMS after being tested for fasting blood glucose levels. Behavioral tests
387 validated the CUMS model, and the T2DM mice with depression-like phenotype mice model
388 was well established. In sucrose preference test, it showed that T2DM mice got lower sucrose
389 preference rate when comparing with Control, which indicated that T2DM mice developed a
390 depression-like phenotype during the course of the disease, just as reported (Hai-Na et al. 2020).
391 In addition, it was found that CUMS exacerbated the depression-like phenotype in diabetic mice.
392 The diabetic mice developed a depression-like phenotype in the development of the disease,
393 which further worsened when CUMS was continued to be given.

394

395 We discovered a bidirectional predisposing risk between T2DM and depression in a 4-week
396 CUMS mouse model. We took serum samples from mice to look for relevant biochemical
397 indicators. Indeed, chronic stress increased CHO, TG, HDL, LDL, and NEFA levels of diabetic
398 mice, while diabetes also increased CHO, TG, LDL, HDL and NEFA levels in stressed mice. It

399 is generally accepted that diabetic mice disturb serum lipid profile with higher TC, TG and LDL-
400 C levels and lower HDL-C level (Manickam et al. 2022). However, the lipid profile of diabetic
401 mice was not unanimously reflected in the literature. Interestingly, in our study, we found that
402 diabetic mice show elevated HDL, which in line with some studies (Ivanovic et al. 2015; Qin et
403 al. 2018).

404

405 Insulin resistance and β cell failure are hallmarks of T2DM(DeFronzo 2009). Insulin resistance is
406 defined as impaired peripheral tissue response to insulin stimulation, resulting in elevated
407 peripheral insulin levels(Polidori et al. 2022). It has a bidirectional causal interaction with
408 depression. Insulin resistance raises the risk of depression and worsens it, and depression raises
409 the risk of insulin resistance and worsens it(Watson et al. 2018). A meta-analysis study found
410 that insulin levels and the HOMA-IR index were higher in patients with acute
411 depression(Fernandes et al. 2022). In our study, stressed mice in the CUMS or T2DM+CUMS
412 groups developed insulin resistance. The main physiological function of β -cells is insulin
413 synthesis and secretion. When pancreatic β -cells are dysfunctional and insulin secretion is
414 lacking, blood glucose levels rise dramatically and diabetes develops gradually. Normal
415 pancreatic β -cells are highly sensitive to changes in blood glucose levels, and a decrease in the
416 number of pancreatic β -cells, whether direct or indirect, can directly lead to impaired insulin
417 secretion and β -cell function(Rorsman & Ashcroft 2018). T2DM+CUMS group comorbid lower
418 HOMA- β index were observed in our studies, as our data indicated. Moreover, the number and
419 area of pancreatic islet β -cells were reduced. The gold standard for assessing the concentration of
420 glycemic control is GHbA1c, which reflects the average blood glucose level over the previous 8-
421 12 weeks. The GHbA1c result revealed that it did not raise the concentration of GHbA1c in the
422 presence of comorbid CUMS.

423

424 Notably, the diabetes and depression comorbidity mice showed decreased levels in HDL and
425 GHbA1c compared to the diabetic mice, although the differences were not significant. We
426 considered that the lower levels of HDL and GHbA1c might influence by some metabolic
427 enzymes associated with lipid accumulation, and the CUMS exposure might play a role in these
428 mechanisms. However, further researches are needed to verify these.

429 According to the results of the liver pathology, liver function, liver weight/body weight ratio and
430 total bile acid level, the T2DM+CUMS group had a worsening degree of lesions such as steatosis
431 and inflammatory cell infiltration compared to T2DM or CUMS, and also increased liver/body
432 weight, ALT or AST, total bile acid level, indicating a disturbance of lipid metabolism after the
433 comorbidity of depression and T2DM.

434

435 Bile acids are relatively strong detergents, and they are potentially toxic to cells. Therefore, the
436 cellular levels of bile acids must be strictly controlled. It was found that FXR is a major regulator
437 of bile acid homeostasis and may have a role in protecting cells from bile acid toxicity. FXR is a
438 nuclear receptor superfamily ligand-activated member that is primarily expressed in the liver and

439 ileum and plays an important role in the development of metabolic diseases(Matsubara et al.
440 2013). FXR activation in the liver has been shown to protect against the development of hepatic
441 steatosis. Hepatic FXR deficiency exacerbates hepatic steatosis in a high cholesterol diet
442 model(Schmitt et al. 2015). FXR activation in the liver reduces hepatic lipid content by
443 decreasing lipogenesis and increasing fatty acid oxidation(Pineda Torra et al. 2003; Watanabe et
444 al. 2004b). FXR^{-/-} mice had increased liver fat accompanied by elevated triglycerides,
445 cholesterol, non-esterified fatty acid and lipoproteins (VLDL and LDL) (Sinal et al. 2000). In
446 contrast, in diabetic (db/db), obese (ob/ob) or wild-type mice, the use of bile acids or FXR
447 agonists reduces plasma triglycerides, fatty acids and cholesterol, as well as reducing hepatic
448 lipid/steatosis (Watanabe et al. 2004b; Zhang et al. 2006). In the present study, we found that
449 reduced hepatic FXR mRNA and protein expression was observed in T2DM+CUMS animal
450 models when compared to T2DM mice, suggesting a possible role for FXR in T2DM or CUMS.
451 Reduced expression of sterol regulatory element binding protein 1c (SREBP1c) by inducing SHP
452 and FXR activation, resulting in decreased expression of adipogenesis-related genes(Watanabe et
453 al. 2004b). In this study, Hepatic FXR protein and mRNA levels were downregulated in
454 T2DM+CUMS groups of mice, while the protein of SHP, the target gene of FXR, in the liver
455 was not significantly different among the T2DM and T2DM+CUMS groups. As opposed to
456 FXR, SHP showed an increased mRNA and protein levels in T2DM+CUMS group than T2DM.
457 In previous study, liver-specific SHP deletion prevents hepatic steatosis and fatty liver
458 development (Akinrotimi et al. 2017). Obviously, CUMS exacerbates hepatic steatosis in
459 diabetic mice possibly through the FXR-SHP pathway. It is suggested that the lipid metabolism
460 disturbance that occurs in diabetic mice after administration of chronic stress-induced
461 depression-like phenotype may be mediated by FXR-SHP pathway.

462
463 FXR influences hepatic glucose metabolism in addition to regulating hepatic lipid levels. FXR
464 activation reduces gluconeogenesis while increasing glycolysis(Ma et al. 2006). Insulin
465 resistance was found in FXR^{-/-} mice at an early stage, suggesting a role for FXR in glucose
466 metabolism (Cariou et al. 2006; Zhang et al. 2006). Consistent with this, in wild-type or diabetic
467 db/db or insulin-resistant ob/ob mice, the use of bile acids or FXR-specific agonists increased
468 insulin sensitivity and reduced blood glucose concentrations (Cariou et al. 2006; Zhang et al.
469 2006). And our results showed the same performance, with downregulation of hepatic FXR
470 protein and mRNA levels in both T2DM and T2DM+CUMS groups of mice. Enterocytes can
471 activate the nuclear receptor FXR, which results in the production of FGF15 (Kliwer &
472 Mangelsdorf 2015). In addition to the enterohepatic cycle, FGF15 can signal in an endocrine
473 manner and is involved in lipid and glucose metabolism (Owen et al. 2015). Previous studies
474 have shown that FGF15 secreted from the ileum after FXR activation has insulin-like effects and
475 inhibits hepatic gluconeogenesis (Kir et al. 2011; Potthoff et al. 2011; Potthoff et al. 2012;
476 Schaap 2012). In the present study, the mRNA and protein expression levels of FGF15 were
477 downregulated in the ileum of both T2DM and T2DM+CUMS groups of mice.

478

479 In the brain, only about 20% of BAs are synthesized locally(Monteiro-Cardoso et al. 2021). BAs
480 acts as a ligand for the nuclear receptor FXR. FXR activation in hippocampal tissue has been
481 linked to neurological disorders. Previous research found that FXR expression is significantly
482 downregulated in the medial prefrontal cortex of mice with a depression-like phenotype caused
483 by chronic social defeat stress (CSDS)(Bao et al. 2021). Similarly, it is entirely consistent with
484 the findings of this study. Simultaneously, there was a downward trend following the depression
485 and T2DM comorbidity. Previous studies have found that FXR expression in the medial
486 prefrontal cortex is significantly downregulated in mice with chronic social defeat stress
487 (CSDS)-induced depression-like phenotype(Bao et al. 2021). In the present study, the results
488 showed that mice in T2DM+CUMS group downregulated the expression of hepatic FXR protein
489 and mRNA while upregulated the expression of hepatic SHP protein and mRNA. While in the
490 ileum, mice in T2DM + CUMS group also downregulated FXR protein and mRNA expression,
491 and the mRNA and protein expression of FGF15 also showed a decreasing trend in the
492 T2DM+CUMS group.

493

494 **Conclusions**

495 To the best of our knowledge, the relationship between the comorbidity of T2DM and depression
496 and activation of FXR or its target genes has not been reported. This study suggests that FXR
497 and its downstream gene FGF15 are critical components in the development of depression-like
498 phenotypes, and it identifies FXR-FGF15 as a potential novel therapeutic target for the treatment
499 of T2DM and depression comorbidity.

500

501 **Conflict of Interest**

502 The authors declare that the research was conducted in the absence of any commercial or
503 financial relationships that could be construed as a potential conflict of interest.

504

505 **Ethics Statement**

506 The animal study was reviewed and approved by The Animal Care and Use Committee in
507 Shanghai Sixth People's Hospital.

508

509 **Author Contributions**

510 Study conception and design: WC, CL and FX; acquisition of data: WC, CL, ZS, JC, ZC, YC
511 and ZG; drafting of the manuscript: WC, CL, FX; critical revision: FX. All authors have read
512 and agreed to the published version of the manuscript.

513

514 **Funding**

515 This work was supported by the Shanghai Municipal Science Commission [grant number
516 19411971700].

517

518 Acknowledgements

519 We are indebted to all the graduate students and postdoctoral fellows.

520

521 References

- 522 Agardh E, Allebeck P, Hallqvist J, Moradi T, and Sidorchuk A. 2011. Type 2 diabetes incidence
523 and socio-economic position: a systematic review and meta-analysis. *Int J Epidemiol*
524 40:804-818. 10.1093/ije/dyr029
- 525 Akinrotimi O, Riessen R, VanDuyne P, Park JE, Lee YK, Wong LJ, Zavacki AM, Schoonjans K,
526 and Anakk S. 2017. Small heterodimer partner deletion prevents hepatic steatosis and
527 when combined with farnesoid X receptor loss protects against type 2 diabetes in mice.
528 *Hepatology* 66:1854-1865. 10.1002/hep.29305
- 529 Ali S, Stone MA, Peters JL, Davies MJ, and Khunti K. 2006. The prevalence of co-morbid
530 depression in adults with Type 2 diabetes: a systematic review and meta-analysis.
531 *Diabet Med* 23:1165-1173. 10.1111/j.1464-5491.2006.01943.x
- 532 Bădescu SV, Tătaru C, Kobylinska L, Georgescu EL, Zahiu DM, Zăgrean AM, and Zăgrean L.
533 2016. The association between Diabetes mellitus and Depression. *J Med Life* 9:120-125.
- 534 Bao H, Li H, Jia Y, Xiao Y, Luo S, Zhang D, Han L, Dai L, Xiao C, Feng L, Feng Y, Yang Y,
535 Wang H, Wang G, and Du J. 2021. Ganoderic acid A exerted antidepressant-like action
536 through FXR modulated NLRP3 inflammasome and synaptic activity. *Biochem*
537 *Pharmacol* 188:114561. 10.1016/j.bcp.2021.114561
- 538 Cariou B, van Harmelen K, Duran-Sandoval D, van Dijk TH, Grefhorst A, Abdelkarim M, Caron
539 S, Torpier G, Fruchart JC, Gonzalez FJ, Kuipers F, and Staels B. 2006. The farnesoid X
540 receptor modulates adiposity and peripheral insulin sensitivity in mice. *J Biol Chem*
541 281:11039-11049. 10.1074/jbc.M510258200
- 542 Caron S, Huaman Samanez C, Dehondt H, Ploton M, Briand O, Lien F, Dorchie E, Dumont J,
543 Postic C, Cariou B, Lefebvre P, and Staels B. 2013. Farnesoid X receptor inhibits the
544 transcriptional activity of carbohydrate response element binding protein in human
545 hepatocytes. *Mol Cell Biol* 33:2202-2211. 10.1128/MCB.01004-12
- 546 Defronzo RA. 2009. Banting Lecture. From the triumvirate to the ominous octet: a new paradigm
547 for the treatment of type 2 diabetes mellitus. *Diabetes* 58:773-795. 10.2337/db09-9028
- 548 Duran-Sandoval D, Cariou B, Percevault F, Hennuyer N, Grefhorst A, van Dijk TH, Gonzalez
549 FJ, Fruchart JC, Kuipers F, and Staels B. 2005. The farnesoid X receptor modulates
550 hepatic carbohydrate metabolism during the fasting-refeeding transition. *J Biol Chem*
551 280:29971-29979. 10.1074/jbc.M501931200
- 552 Egede LE, and Ellis C. 2010. Diabetes and depression: global perspectives. *Diabetes Res Clin*
553 *Pract* 87:302-312. 10.1016/j.diabres.2010.01.024
- 554 Feng L, Zhou N, Li Z, Fu D, Guo Y, Gao X, and Liu X. 2022. Co-occurrence of gut microbiota
555 dysbiosis and bile acid metabolism alteration is associated with psychological disorders
556 in Crohn's disease. *Faseb j* 36:e22100. 10.1096/fj.202101088RRR
- 557 Fernandes BS, Salagre E, Enduru N, Grande I, Vieta E, and Zhao Z. 2022. Insulin resistance in
558 depression: A large meta-analysis of metabolic parameters and variation. *Neurosci*
559 *Biobehav Rev* 139:104758. 10.1016/j.neubiorev.2022.104758
- 560 Fisher EB, Chan JCN, Nan H, Sartorius N, and Oldenburg B. 2012. Co-occurrence of diabetes
561 and depression: Conceptual considerations for an emerging global health challenge.
562 *Journal of Affective Disorders* 142:S56-S66. 10.1016/s0165-0327(12)70009-5
- 563 Fisher L, Skaff MM, Mullan JT, Arean P, Glasgow R, and Masharani U. 2008. A longitudinal
564 study of affective and anxiety disorders, depressive affect and diabetes distress in adults
565 with Type 2 diabetes. *Diabet Med* 25:1096-1101. 10.1111/j.1464-5491.2008.02533.x

- 566 Furman BL. 2021. Streptozotocin-Induced Diabetic Models in Mice and Rats. *Curr Protoc* 1:e78.
567 10.1002/cpz1.78
- 568 Gilbert ER, Fu Z, and Liu D. 2011. Development of a nongenetic mouse model of type 2
569 diabetes. *Exp Diabetes Res* 2011:416254. 10.1155/2011/416254
- 570 Hai-Na Z, Xu-Ben Y, Cong-Rong T, Yan-Cheng C, Fan Y, Lei-Mei X, Ruo-Lan S, Ye Z, Ye-Xuan
571 W, and Jing L. 2020. Atorvastatin ameliorates depressive behaviors and
572 neuroinflammatory in streptozotocin-induced diabetic mice. *Psychopharmacology (Berl)*
573 237:695-705. 10.1007/s00213-019-05406-w
- 574 Harding JL, Pavkov ME, Magliano DJ, Shaw JE, and Gregg EW. 2019a. Global trends in
575 diabetes complications: a review of current evidence. *Diabetologia* 62:3-16.
576 10.1007/s00125-018-4711-2
- 577 Harding KA, Pushpanathan ME, Whitworth SR, Nanthakumar S, Bucks RS, and Skinner TC.
578 2019b. Depression prevalence in Type 2 diabetes is not related to diabetes-depression
579 symptom overlap but is related to symptom dimensions within patient self-report
580 measures: a meta-analysis. *Diabet Med* 36:1600-1611. 10.1111/dme.14139
- 581 Heckbert SR, Rutter CM, Oliver M, Williams LH, Ciechanowski P, Lin EH, Katon WJ, and Von
582 Korff M. 2010. Depression in relation to long-term control of glycemia, blood pressure,
583 and lipids in patients with diabetes. *J Gen Intern Med* 25:524-529. 10.1007/s11606-010-
584 1272-6
- 585 Huang F, Wang T, Lan Y, Yang L, Pan W, Zhu Y, Lv B, Wei Y, Shi H, Wu H, Zhang B, Wang J,
586 Duan X, Hu Z, and Wu X. 2015. Deletion of mouse FXR gene disturbs multiple
587 neurotransmitter systems and alters neurobehavior. *Front Behav Neurosci* 9:70.
588 10.3389/fnbeh.2015.00070
- 589 Ivanovic N, Minic R, Dimitrijevic L, Radojevic Skodric S, Zivkovic I, and Djordjevic B. 2015.
590 *Lactobacillus rhamnosus* LA68 and *Lactobacillus plantarum* WCFS1 differently influence
591 metabolic and immunological parameters in high fat diet-induced hypercholesterolemia
592 and hepatic steatosis. *Food Funct* 6:558-565. 10.1039/c4fo00843j
- 593 Kir S, Beddow SA, Samuel VT, Miller P, Previs SF, Suino-Powell K, Xu HE, Shulman GI,
594 Kliever SA, and Mangelsdorf DJ. 2011. FGF19 as a postprandial, insulin-independent
595 activator of hepatic protein and glycogen synthesis. *Science* 331:1621-1624.
596 10.1126/science.1198363
- 597 Kiriya Y, and Noshi H. 2019. The Biosynthesis, Signaling, and Neurological Functions of Bile
598 Acids. *Biomolecules* 9. 10.3390/biom9060232
- 599 Kliever SA, and Mangelsdorf DJ. 2015. Bile Acids as Hormones: The FXR-FGF15/19 Pathway.
600 *Dig Dis* 33:327-331. 10.1159/000371670
- 601 Lim GY, Tam WW, Lu Y, Ho CS, Zhang MW, and Ho RC. 2018. Prevalence of Depression in
602 the Community from 30 Countries between 1994 and 2014. *Sci Rep* 8:2861.
603 10.1038/s41598-018-21243-x
- 604 Lin EH, Katon W, Rutter C, Simon GE, Ludman EJ, Von Korff M, Young B, Oliver M,
605 Ciechanowski PC, Kinder L, and Walker E. 2006. Effects of enhanced depression
606 treatment on diabetes self-care. *Ann Fam Med* 4:46-53. 10.1370/afm.423
- 607 Lirong W, Mingliang Z, Mengci L, Qihao G, Zhenxing R, Xiaojiao Z, and Tianlu C. 2022. The
608 clinical and mechanistic roles of bile acids in depression, Alzheimer's disease, and
609 stroke. *Proteomics* 22:e2100324. 10.1002/pmic.202100324
- 610 Luo J QJ, Tsai J, Hobensack CK, Sullivan C, Hector R, et al. 1998. Nongenetic mouse models
611 of non-insulin-dependent diabetes mellitus. *Metabolism* 47:663-668.
- 612 Ma K, Saha PK, Chan L, and Moore DD. 2006. Farnesoid X receptor is essential for normal
613 glucose homeostasis. *J Clin Invest* 116:1102-1109. 10.1172/jci25604
- 614 Manickam R, Tur J, Badole SL, Chapalamadugu KC, Sinha P, Wang Z, Russ DW, Brotto M,
615 and Tipparaju SM. 2022. Namp1 activator P7C3 ameliorates diabetes and improves

- 616 skeletal muscle function modulating cell metabolism and lipid mediators. *J Cachexia*
617 *Sarcopenia Muscle* 13:1177-1196. 10.1002/jcsm.12887
- 618 Matsubara T, Li F, and Gonzalez FJ. 2013. FXR signaling in the enterohepatic system. *Mol Cell*
619 *Endocrinol* 368:17-29. 10.1016/j.mce.2012.05.004
- 620 Mertens KL, Kalsbeek A, Soeters MR, and Eggink HM. 2017. Bile Acid Signaling Pathways from
621 the Enterohepatic Circulation to the Central Nervous System. *Frontiers in Neuroscience*
622 11. 10.3389/fnins.2017.00617
- 623 Monteiro-Cardoso VF, Corliano M, and Singaraja RR. 2021. Bile Acids: A Communication
624 Channel in the Gut-Brain Axis. *Neuromolecular Med* 23:99-117. 10.1007/s12017-020-
625 08625-z
- 626 Moulton CD, Pickup JC, and Ismail K. 2015. The link between depression and diabetes: the
627 search for shared mechanisms. *Lancet Diabetes Endocrinol* 3:461-471. 10.1016/s2213-
628 8587(15)00134-5
- 629 Nollet M. 2021. Models of Depression: Unpredictable Chronic Mild Stress in Mice. *Curr Protoc*
630 1:e208. 10.1002/cpz1.208
- 631 Owen BM, Mangelsdorf DJ, and Kliewer SA. 2015. Tissue-specific actions of the metabolic
632 hormones FGF15/19 and FGF21. *Trends Endocrinol Metab* 26:22-29.
633 10.1016/j.tem.2014.10.002
- 634 Perino A, and Schoonjans K. 2022. Metabolic Messengers: bile acids. *Nat Metab* 4:416-423.
635 10.1038/s42255-022-00559-z
- 636 Petrak F, Baumeister H, Skinner TC, Brown A, and Holt RIG. 2015. Depression and diabetes:
637 treatment and health-care delivery. *Lancet Diabetes Endocrinol* 3:472-485.
638 10.1016/s2213-8587(15)00045-5
- 639 Pineda Torra I, Claudel T, Duval C, Kosykh V, Fruchart JC, and Staels B. 2003. Bile acids
640 induce the expression of the human peroxisome proliferator-activated receptor alpha
641 gene via activation of the farnesoid X receptor. *Mol Endocrinol* 17:259-272.
642 10.1210/me.2002-0120
- 643 Podrini C, Cambridge EL, Lelliott CJ, Carragher DM, Estabel J, Gerdin AK, Karp NA,
644 Scudamore CL, Sanger Mouse Genetics P, Ramirez-Solis R, and White JK. 2013. High-
645 fat feeding rapidly induces obesity and lipid derangements in C57BL/6N mice. *Mamm*
646 *Genome* 24:240-251. 10.1007/s00335-013-9456-0
- 647 Polidori N, Mainieri F, Chiarelli F, Mohn A, and Giannini C. 2022. Early Insulin Resistance, Type
648 2 Diabetes, and Treatment Options in Childhood. *Horm Res Paediatr* 95:149-166.
649 10.1159/000521515
- 650 Potthoff MJ, Boney-Montoya J, Choi M, He T, Sunny NE, Satapati S, Suino-Powell K, Xu HE,
651 Gerard RD, Finck BN, Burgess SC, Mangelsdorf DJ, and Kliewer SA. 2011. FGF15/19
652 regulates hepatic glucose metabolism by inhibiting the CREB-PGC-1 α pathway. *Cell*
653 *Metab* 13:729-738. 10.1016/j.cmet.2011.03.019
- 654 Potthoff MJ, Kliewer SA, and Mangelsdorf DJ. 2012. Endocrine fibroblast growth factors 15/19
655 and 21: from feast to famine. *Genes Dev* 26:312-324. 10.1101/gad.184788.111
- 656 Qin Z, Wang W, Liao D, Wu X, and Li X. 2018. UPLC-Q/TOF-MS-Based Serum Metabolomics
657 Reveals Hypoglycemic Effects of *Rehmannia glutinosa*, *Coptis chinensis* and Their
658 Combination on High-Fat-Diet-Induced Diabetes in KK-Ay Mice. *Int J Mol Sci* 19.
659 10.3390/ijms19123984
- 660 Rorsman P, and Ashcroft FM. 2018. Pancreatic β -Cell Electrical Activity and Insulin Secretion:
661 Of Mice and Men. *Physiol Rev* 98:117-214. 10.1152/physrev.00008.2017
- 662 Roy T, and Lloyd CE. 2012. Epidemiology of depression and diabetes: a systematic review. *J*
663 *Affect Disord* 142 Suppl:S8-21. 10.1016/s0165-0327(12)70004-6
- 664 Sartorius N. 2018. Depression and diabetes. *Dialogues Clin Neurosci* 20:47-52.
665 10.31887/DCNS.2018.20.1/nsartorius

- 666 Schaap FG. 2012. Role of fibroblast growth factor 19 in the control of glucose homeostasis.
667 *Curr Opin Clin Nutr Metab Care* 15:386-391. 10.1097/MCO.0b013e3283547171
- 668 Schmitt J, Kong B, Stieger B, Tschopp O, Schultze SM, Rau M, Weber A, Müllhaupt B, Guo GL,
669 and Geier A. 2015. Protective effects of farnesoid X receptor (FXR) on hepatic lipid
670 accumulation are mediated by hepatic FXR and independent of intestinal FGF15 signal.
671 *Liver Int* 35:1133-1144. 10.1111/liv.12456
- 672 Semenkovich K, Brown ME, Svrakic DM, and Lustman PJ. 2015. Depression in type 2 diabetes
673 mellitus: prevalence, impact, and treatment. *Drugs* 75:577-587. 10.1007/s40265-015-
674 0347-4
- 675 Shao M, Lu X, Cong W, Xing X, Tan Y, Li Y, Li X, Jin L, Wang X, Dong J, Jin S, Zhang C, and
676 Cai L. 2014. Multiple low-dose radiation prevents type 2 diabetes-induced renal damage
677 through attenuation of dyslipidemia and insulin resistance and subsequent renal
678 inflammation and oxidative stress. *PLoS One* 9:e92574. 10.1371/journal.pone.0092574
- 679 Sinal CJ, Tohkin M, Miyata M, Ward JM, Lambert G, and Gonzalez FJ. 2000. Targeted
680 disruption of the nuclear receptor FXR/BAR impairs bile acid and lipid homeostasis. *Cell*
681 102:731-744. 10.1016/s0092-8674(00)00062-3
- 682 Sonne DP, van Nierop FS, Kulik W, Soeters MR, Vilsbøll T, and Knop FK. 2016. Postprandial
683 Plasma Concentrations of Individual Bile Acids and FGF-19 in Patients With Type 2
684 Diabetes. *J Clin Endocrinol Metab* 101:3002-3009. 10.1210/jc.2016-1607
- 685 Sun H, Saeedi P, Karuranga S, Pinkepank M, Ogurtsova K, Duncan BB, Stein C, Basit A, Chan
686 JCN, Mbanya JC, Pavkov ME, Ramachandaran A, Wild SH, James S, Herman WH,
687 Zhang P, Bommer C, Kuo S, Boyko EJ, and Magliano DJ. 2022. IDF Diabetes Atlas:
688 Global, regional and country-level diabetes prevalence estimates for 2021 and
689 projections for 2045. *Diabetes Res Clin Pract* 183:109119.
690 10.1016/j.diabres.2021.109119
- 691 Sun L, Xie C, Wang G, Wu Y, Wu Q, Wang X, Liu J, Deng Y, Xia J, Chen B, Zhang S, Yun C,
692 Lian G, Zhang X, Zhang H, Bisson WH, Shi J, Gao X, Ge P, Liu C, Krausz KW, Nichols
693 RG, Cai J, Rimal B, Patterson AD, Wang X, Gonzalez FJ, and Jiang C. 2018. Gut
694 microbiota and intestinal FXR mediate the clinical benefits of metformin. *Nat Med*
695 24:1919-1929. 10.1038/s41591-018-0222-4
- 696 Sun W, Zhang D, Wang Z, Sun J, Xu B, Chen Y, Ding L, Huang X, Lv X, Lu J, Bi Y, and Xu Q.
697 2016. Insulin Resistance is Associated With Total Bile Acid Level in Type 2 Diabetic and
698 Nondiabetic Population: A Cross-Sectional Study. *Medicine (Baltimore)* 95:e2778.
699 10.1097/md.0000000000002778
- 700 Vancampfort D, Correll CU, Gallinger B, Probst M, De Hert M, Ward PB, Rosenbaum S,
701 Gaughran F, Lally J, and Stubbs B. 2016. Diabetes mellitus in people with
702 schizophrenia, bipolar disorder and major depressive disorder: a systematic review and
703 large scale meta-analysis. *World Psychiatry* 15:166-174. 10.1002/wps.20309
- 704 Viigimaa M, Sachinidis A, Toumpourleka M, Koutsampasopoulos K, Alliksoo S, and Titma T.
705 2020. Macrovascular Complications of Type 2 Diabetes Mellitus. *Curr Vasc Pharmacol*
706 18:110-116. 10.2174/1570161117666190405165151
- 707 Watanabe M, Houten SM, Wang L, Moschetta A, Mangelsdorf DJ, Heyman RA, Moore DD, and
708 Auwerx J. 2004a. Bile acids lower triglyceride levels via a pathway involving FXR, SHP,
709 and SREBP-1c. *Journal of Clinical Investigation* 113:1408-1418. 10.1172/jci200421025
- 710 Watanabe M, Houten SM, Wang L, Moschetta A, Mangelsdorf DJ, Heyman RA, Moore DD, and
711 Auwerx J. 2004b. Bile acids lower triglyceride levels via a pathway involving FXR, SHP,
712 and SREBP-1c. *J Clin Invest* 113:1408-1418. 10.1172/jci21025
- 713 Watson K, Nasca C, Aasly L, McEwen B, and Rasgon N. 2018. Insulin resistance, an unmasked
714 culprit in depressive disorders: Promises for interventions. *Neuropharmacology* 136:327-
715 334. 10.1016/j.neuropharm.2017.11.038

- 716 Yan N, Yan T, Xia Y, Hao H, Wang G, and Gonzalez FJ. 2021. The pathophysiological function
717 of non-gastrointestinal farnesoid X receptor. *Pharmacol Ther* 226:107867.
718 10.1016/j.pharmthera.2021.107867
- 719 Zhang F, Jia Z, Gao P, Kong H, Li X, Lu X, Wu Y, and Xu G. 2010. Metabonomics study of urine
720 and plasma in depression and excess fatigue rats by ultra fast liquid chromatography
721 coupled with ion trap-time of flight mass spectrometry. *Mol Biosyst* 6:852-861.
722 10.1039/b914751a
- 723 Zhang Y, Lee FY, Barrera G, Lee H, Vales C, Gonzalez FJ, Willson TM, and Edwards PA. 2006.
724 Activation of the nuclear receptor FXR improves hyperglycemia and hyperlipidemia in
725 diabetic mice. *Proc Natl Acad Sci U S A* 103:1006-1011. 10.1073/pnas.0506982103
- 726 Zhu YL, Li SL, Zhu CY, Wang W, Zuo WF, and Qiu XJ. 2020. Metabolomics analysis of the
727 antidepressant prescription Danzhi Xiaoyao Powder in a rat model of Chronic
728 Unpredictable Mild Stress (CUMS). *J Ethnopharmacol* 260:112832.
729 10.1016/j.jep.2020.112832
730

Figure 1

Type 2 diabetic mice with depression-like phenotype comorbidity model validation

(A) Schedule of T2DM and chronic stress induced depression-like phenotype comorbidity model establishment. (B) Total distance, central distance and central durations in open field test, as well as the tracking map. (C) Immobility durations in tail suspension test. (D) Immobility durations in forced swimming test. (E) Sucrose preference rate in sucrose preference test. Data presented as mean \pm SEM, n=10 per group. $^{##}P<0.01$ compared with the Control group, $^{*}P<0.05$, $^{**}P<0.01$ compared with the T2DM+CUMS group.

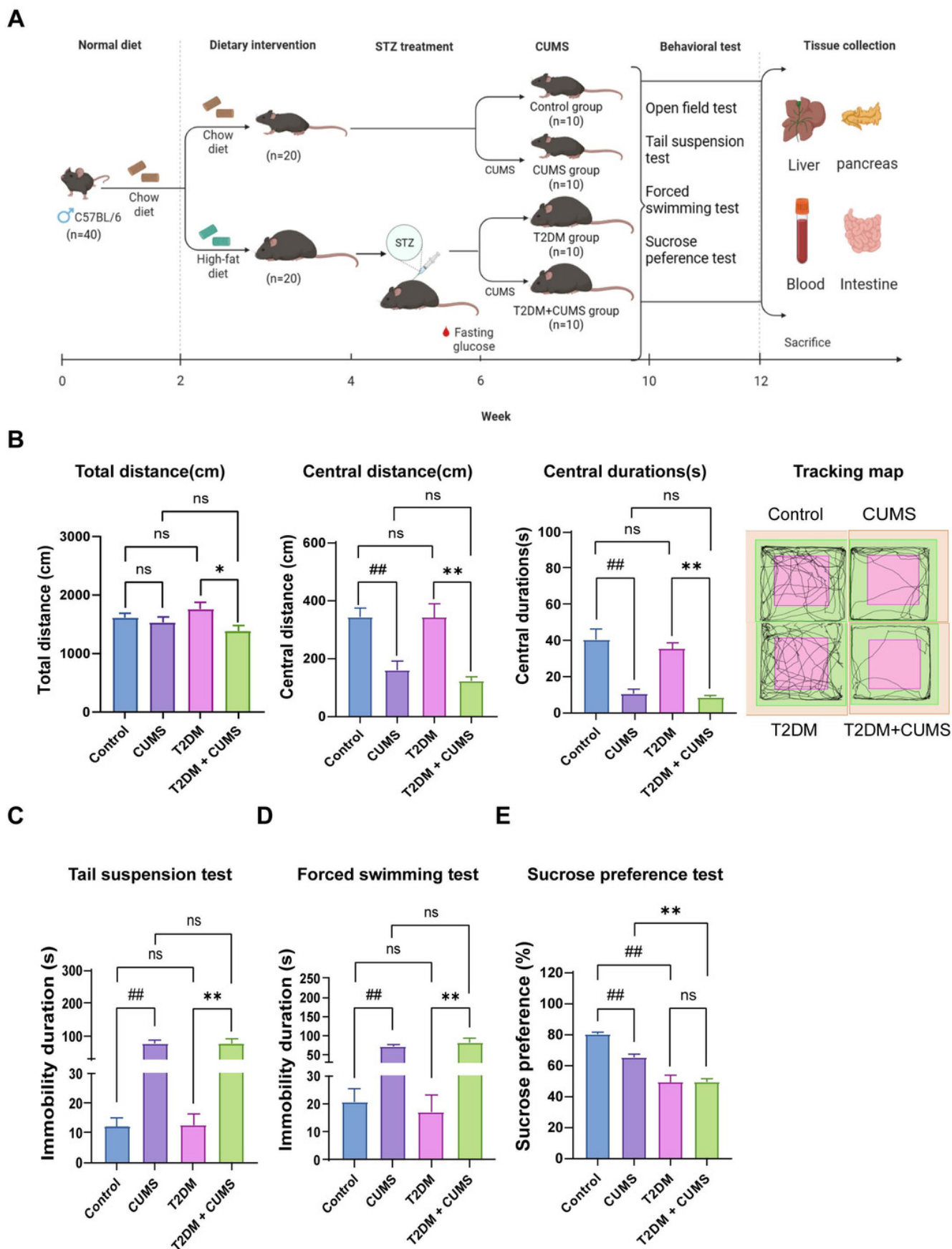


Table 1 (on next page)

The schedule of stressors.

1 **Appendix-table 1. The schedule of stressors.**

2

					Cage	Damp
					vibration	sawdust
					Restraint	Cage
					stress	tilting
	Swimmin					Swimmin
Noise	g at 4°C	Cage	Restraint	Damp	No	g at 4°C
No	Cycle	tilting	stress	sawdust	sawdust	Cycle
sawdust	disturban	Noise	Cage	Noise	Noise	disturban
	ces		vibration			ces
Restraint	Swimmin		Restraint	Cycle	Swimmin	Restraint
stress	g at 4°C	Cage	stress	disturban	g at 4°C	stress
Cage	Cycle	tilting	Cage	ce	Cycle	Cage
vibration	disturban	Noise	vibration	Noise	disturban	vibration
	ces				ces	
Cage		No	Cage		Restraint	
vibration	Damp	sawdust	tilting	Swimmin	stress	Noise
Cycle	sawdust	Cage	Cycle	g at 4°C	Cage	Cage
disturban	Noise	vibration	disturban	Noise	vibration	tilting
ces			ces			

Swimmin	Restraint		Damp	
g at 4°C	stress	Cage	sawdust	No
Cycle	Cage	tilting	Restraint	sawdust
disturban	vibration	Noise	stress	Noise
ces				

Table 2 (on next page)

List of qPCR primer sequences.

1 **Appendix-table 2. List of qPCR primer sequences.**

Genes	Forward primer (5'→3')	Reverse primer (5'→3')
FXR	ATGGCAACCAGTCATGTACAGA	ATTGAAAATCTCCGCCGAACGA
SHP	TAGATCTCTTCTTCCGCCCTA	AGACTCCATTCCACGGGTCA
FGF15	GACTGCGAGGAGGACCAAAA	CAGCCCGTATATCTTGCCGT
ACTB	CATCCGTAAAGACCTCTATGCCAAC	ATGGAGCCACCGATCCACA

2

3 *FXR*, farnesoid X receptor; *SHP*, small heterodimer partner; *FGF15*, fibroblast growth factor 15; *ACTB*, β-

4 actin.

5

Figure 2

Type 2 diabetic mice with depression-like phenotype in glycolipid metabolism.

(A) Body weight weekly in CUMS procedures. (B) Body weight in mice after CUMS procedures. (C) Random blood glucose weekly in CUMS procedures. (D) Fasting blood glucose after CUMS procedures. (E) Serum CHO in mice. (F) Serum TG in mice. (G) Serum NEFA in mice. (H) Serum LDL in mice. (I) Serum HDL in mice. (J) GHbA1c in mice. Data presented as mean \pm SEM, $n=10$ per group, $^{\#}P<0.05$, $^{\#\#}P<0.01$ compared with the Control group, $^*P<0.05$, $^{**}P<0.01$ compared with the T2DM+CUMS group.

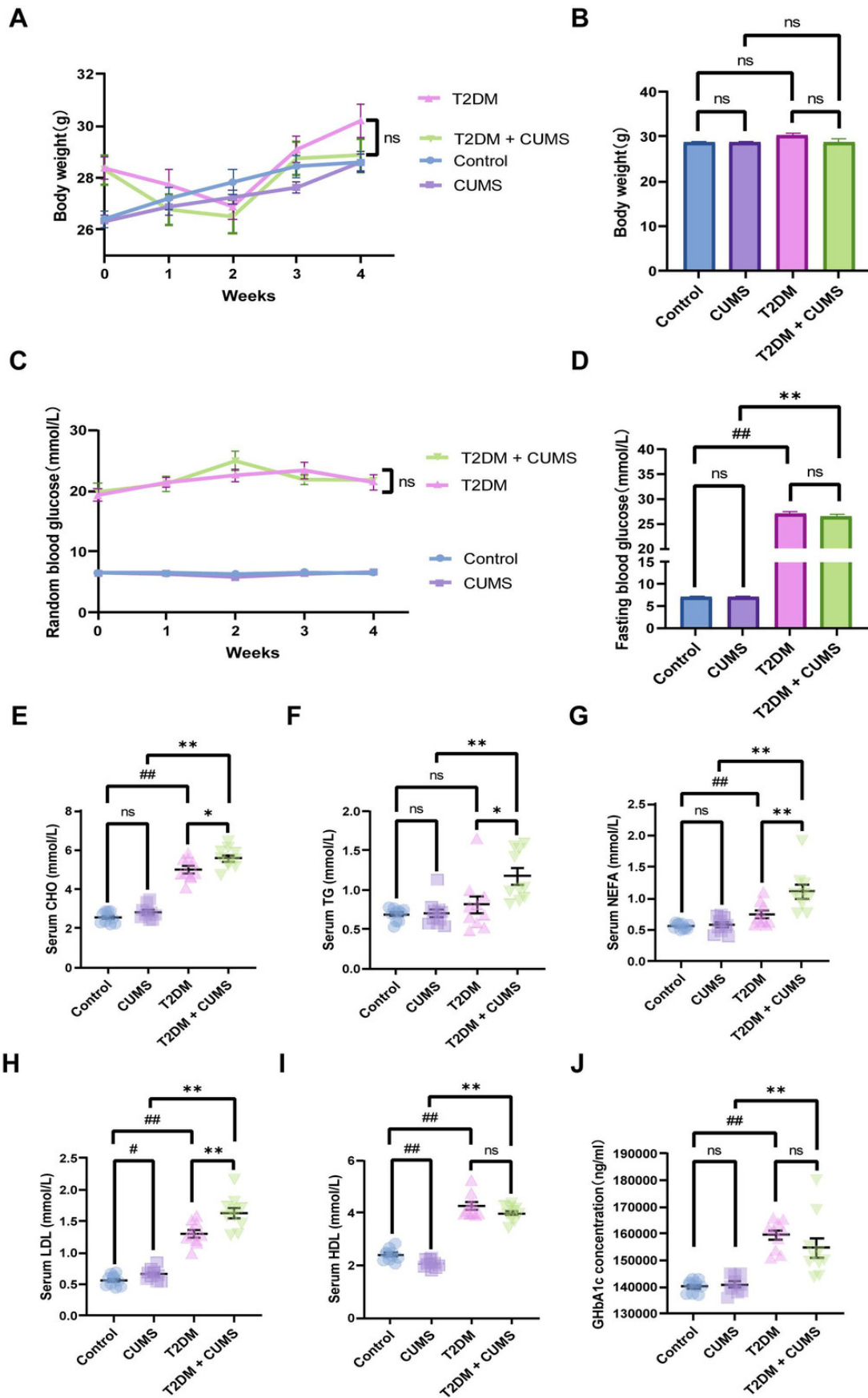


Figure 3

Insulin-related indicators and histopathological analysis of the pancreas in type 2 diabetic mice with depression-like phenotype.

(A) Serum glucose in mice. (B) FINS in mice; (C) HOMA-IR index in mice; (D) HOMA- β index in mice. (E) Representative images of pancreas sections from four groups of mice stained with H&E. Data presented as mean \pm SEM, n=10 per group. $^{\#}P<0.05$, $^{\#\#}P<0.01$ compared with the Control group, $^{**}P<0.01$ compared with the T2DM+CUMS group. Images were taken at 200 \times or 400 \times magnification.

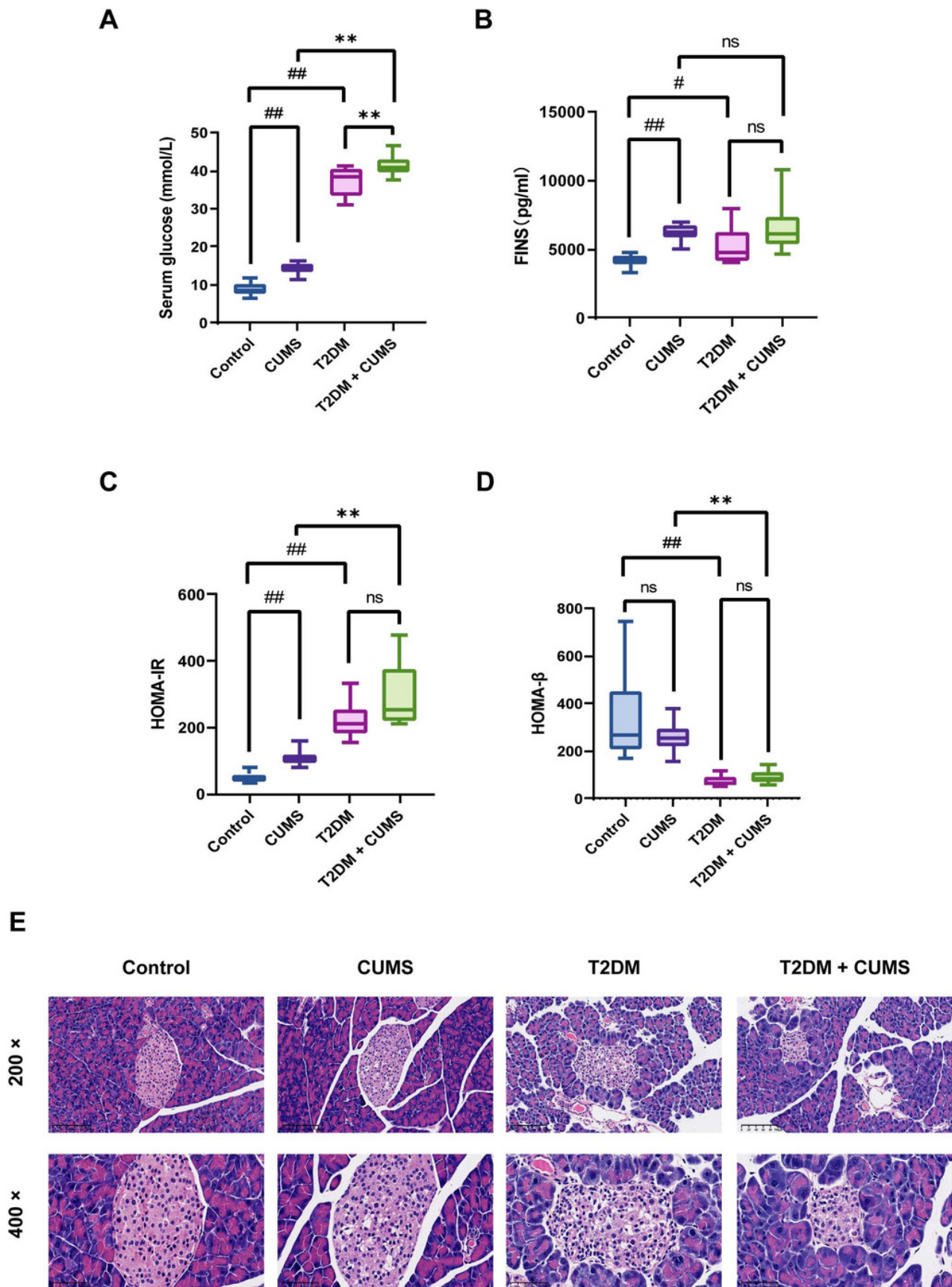


Figure 4

Liver function, total bile acids and histopathological analysis of the liver in type 2 diabetic mice with depression-like phenotype.

(A) Representative images of liver sections from four groups of mice stained with H&E. (B) Lobular inflammation score in four groups. (C) Steatosis score in four groups. (D) Representative images of liver sections from four groups of mice stained with Oil Red O. (E) Hepatic lipids percentage in four group. (F) Liver weight/body weight ratio in mice. (G) ALT level in mice. (H) AST level in mice. (I) Total bile acid level in mice. Data presented as mean \pm SEM, $n=10$. $^{\#}P<0.05$, $^{\#\#}P<0.01$ compared with the Control group, $^*P<0.01$, $^{**}P<0.01$ compared with the T2DM+CUMS group. Images were taken at 10 \times magnification.

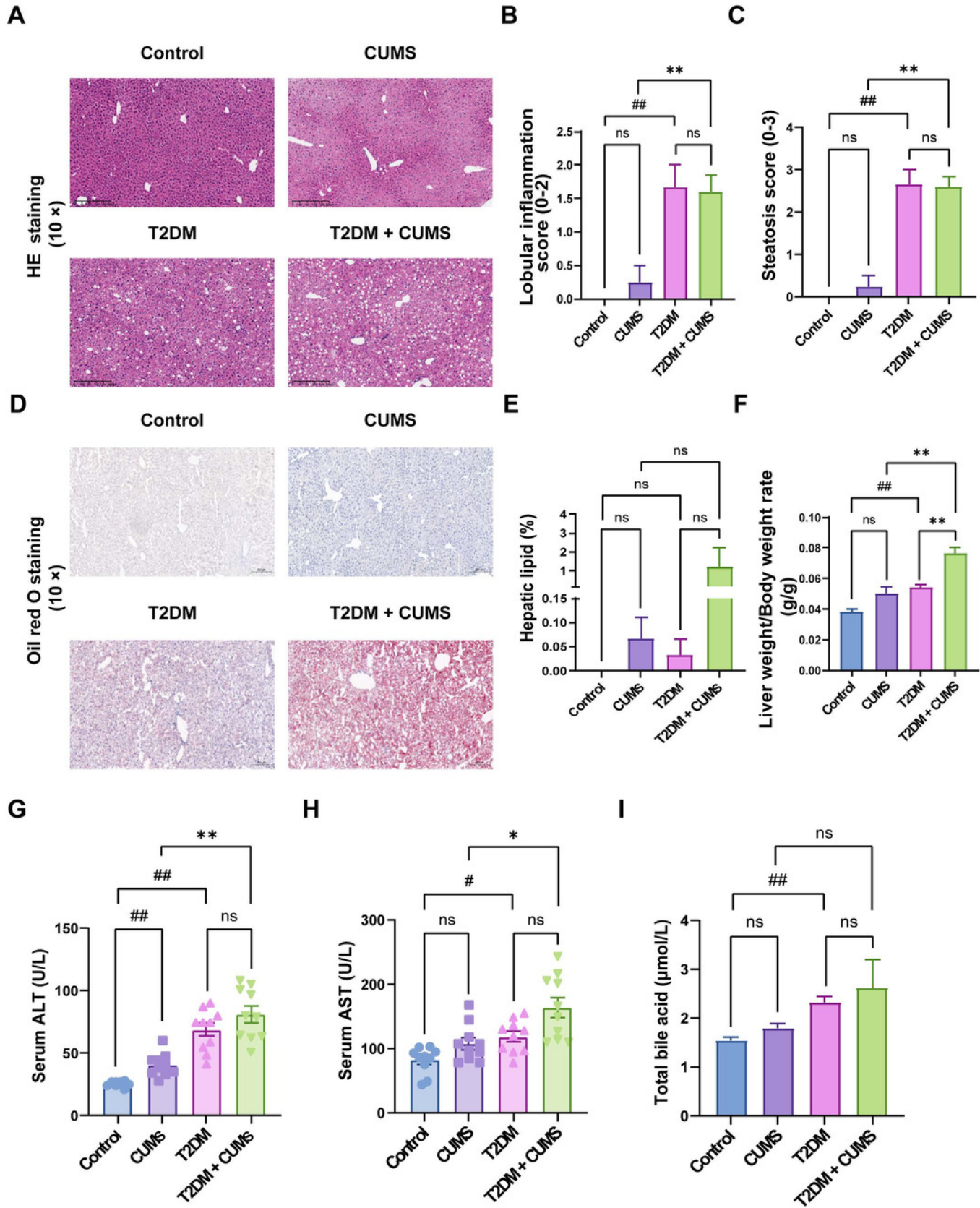


Figure 5

T2DM and depression-like phenotype regulated by FXR/SHP/FGF15.

(A) Relative expression of FXR mRNAs in the livers of mice. (B) Relative expression of SHP mRNAs in the livers of mice. (C) Relative expression of FXR and its target gene SHP proteins in the livers of mice. (D) Relative expression of FXR mRNAs in the ileum of mice. (E) Relative expression of FGF15 mRNAs in the ileum of mice. (F) Relative expression of FXR and its target gene FGF15 proteins in the ileum of mice. Data presented as mean \pm SEM. * $P < 0.05$, ** $P < 0.01$ compared with the T2DM group.

